

# Structural Integrity Assessment of Pressure Vessels with Defect in Welded Joints

Vencislav Grabulov, PhD (Eng)<sup>1)</sup>  
 Stojan Sedmak, PhD (Eng)<sup>2)</sup>  
 Aleksandar Sedmak, PhD (Eng)<sup>3)</sup>  
 Zijah Burzić, PhD (Eng)<sup>1)</sup>

The examples of practical application of fracture mechanics parameters in cracked pressure vessel structural integrity are presented.

The application of fracture mechanics depends on available data, material behaviour, environmental effect and loading. In predominantly static loading material behaviour can be described as linear elastic, based on the stress intensity factor,  $K_I$ , when its ductility is negligible, and as elastic-plastic, with crack opening displacement or the J integral as parameters.

Linear elastic fracture mechanics was applied in a typical service problem when non-allowable defects according to ISO 5817 had been detected by non-destructive testing in regular in-service inspection in welded joints on the cylindrical storage tanks for pressurized air. The defects have been replaced by corresponding cracks for conservative estimate. Simplified application of the stress intensity factor as a parameter and a two parameter fracture assessment diagram from PD6493 Procedure have shown that structural integrity of the analyzed storage tanks is not endangered.

For the detailed elastic-plastic analysis the J integral is used. The experimental pressure vessel was manufactured by welding high strength steel (yield stress 700 MPa) and then precracked artificially for J integral direct measurement.

The theoretical and experimental analyses can not fully describe the behaviour of the cracked welded joint and its heterogenous microstructure. For that purpose, the numerical analysis can be helpful, if applied in a proper way. An example of the finite elements numerical analysis of welded joints is presented.

*Key words:* structural integrity, pressure vessels, welded joint, welded defects, crack, fracture mechanics, stress intensity, j integral, method of finite elements.

## Introduction

THE structural integrity and operational safety of welded pressure vessels primarily depends on weldment behaviour. All efforts in material production and improvements in welding techniques, together with strict requirements for quality assurance, can not exclude the appearance of some imperfections and defects or the formation of cracks during fabrication, stress relieving, hydrostatic proof tests or in service. The possibility of defects and cracks occurrence in welded structures must be recognized, thereby making the use of fracture mechanics analyses inevitable [1].

The development of fracture mechanics enabled the assessment of structural integrity and fitness for service of defective structures. Welding is defined as a "special process" in standards because the welded joints quality can not be verified on the product but has to be built-in in the product. Standard ISO 3834 defines quality requirements for welding. Since welding is a "special process" some imperfections in welds can be accepted, as defined by the acceptability criteria in ISO 5817 "Guidance on quality levels for imperfections". It indicates that cracks, most

severe defects in welded joints, are not allowed, except cracks in the crater of low quality welded joints and microcracks of less than 1 mm<sup>2</sup> cross section. It is not possible to detect reliable cracks of that size by available equipment for nondestructive testing, what means that equipment can operate in real conditions with such imperfections.

The fracture mechanics parameters (stress intensity factor -  $K_I$ , crack opening displacement - COD, J integral) and standardized test methods and procedures for their assessment have provided a new possibility for evaluation of crack significance in a structure. Fracture mechanics is based on homogeneous continuum and uniform material microstructure and properties and thus not directly applicable to welded joints [2]. Published document PD 6493 [3] and SINTAP (Structural Integrity Assessment Procedure) [4], [5] are based on fracture mechanics analyses and experience with cracks in welded structures [6], [7]. The fracture mechanics approach was applied with success in the case of Trans Alaska Crude Oil Pipeline [8], when for the first time the "fitness-for-purpose" approach has been formally accepted, saving significant amount of

<sup>1)</sup> Military Technical Institute (VTI), Ratka Resanovića 1, 11132 Belgrade, SERBIA

<sup>2)</sup> Faculty of Technology and Metallurgy, 11000 Belgrade, SERBIA

<sup>3)</sup> Faculty of mechanical Engineering, 11000 Belgrade, SERBIA

money required for cracks repair. In this case fracture mechanics parameters were accepted as valid, instead of conservative standards for allowable defects. Significant cost for repair of a large number of defects in circumferential welded joints, detected by non-destructive inspection, posed the question of its necessity, since in the pipeline circumferential welded joints are not critical. The responsible institution, according to the requirements of pipeline manufacturer, asked for the help of the U.S.A. National Institute of Standards – NBS (now National Institute of Standards and Technology – NIST). The detailed analysis of the crack opening displacement (COD) considered the crack driving force, on one side, and the crack resistance of welded joints, on the other side. The results of this investigation was formally accepted, and unnecessary costs were avoided. Probably the most important conclusion in this investigation is that the fracture mechanics analysis is an acceptable basis for an allowable exception from valid standards under circumstances, under condition that this analysis provides a clear and conservative structural integrity assessment”.

Heterogeneity has an important role in welded joints behaviour, particularly should high stresses cause local plastic strain [9]. The heat-affected-zone (HAZ) of heterogeneous microstructure and non-uniform properties can be a weak point because its deformation can be constrained and plane strain conditions can prevail. The situation is most complex when an undermatching effect is used to prevent cold cracking [10]. In that case plastic strains are localized in the weld metal until its strain hardening is partly or fully exhausted, when the base metal could start to yield.

Fracture mechanics tests can not be applied with full success to welded joints, because of the heterogeneity of microstructure and properties, especially if the HAZ is to be examined.

The main role of fracture mechanics is to link in a proper way three variables: stress, defect size and fracture toughness.

### Example of cylindrical storage tanks structural integrity assessment

This example presents a typical problem when non-allowable defects according to ISO 5817 were detected by the non-destructive testing during a regular in-service inspection in the welded joints of the several storage tanks for pressurized air (Fig.1) at the Hydro-Electrical Power Plant “Bajina Bašta” [11]. Three non-allowable defects were detected by radiography on pressure vessel 974. All of them were distributed on a circumferential welded joint. Two of them belonged to form imperfections (undercut - defect 501 according to ISO 5817), and their effect can be neglected, because of low applied stress. They can be easily removed by grinding, followed by only small reduction of wall thickness, with no effect on pressure vessel structural integrity. The defect 970-64 was additionally inspected ultrasonically and described as a lack of penetration 60 mm long and 2 mm wide. Here, the dimension in the direction of the welded joint is taken as the defect length (longitudinal welded joint, close to the circumferential welded joint between the cylindrical mantle and the torispherical lid), and its width as the dimension in direction of the weld width. The pressure vessel 978 contained five non-allowable defects. Lack of penetration (978-14), 25 mm long, was selected as critical (Fig.1),

although re-inspection by ultrasonic testing did not reveal any defect found by radiography. The width of this defect was taken to be 2 mm, the size corresponding to the weld root size according to the design of the pressure vessel 978, and in the same time being the upper sensitivity limit of ultrasonic testing. Overlapping 57, 10 mm long, in the middle of the circumferential weld on the pressure vessel 971 was also selected as critical (Fig.1).

According to standards, further service of equipment containing non-allowable defects is not permitted, and fitness-for-service is required.

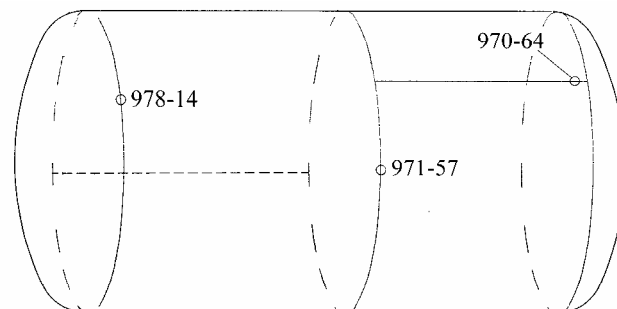


Figure 1. Presentation of the defects position on the cylindrical storage tanks for pressurized air

Following the approach, applied in the case of the Alaska pipeline, further service of the pressure vessel can be allowed by the Inspection Office if structural integrity is not endangered by the presence of detected defects. Three arguments supported this approach. The first argument was that the inspected pressure vessels were in service for more than 30 years, without any problems. The second argument was that previous inspections were not so rigorous, and had been performed with less sensitive equipment. The third argument was that standards and codes nowadays are more strict than corresponding standards and codes used in time of design and previous service. Still it was necessary to prove structural integrity of pressure vessels in the conservative way. Load was quasi-static pressure, with no environment or temperature effects. The most probable failure mode could be brittle fracture, indicating the necessity to apply linear elastic fracture mechanics (LEFM) in structural integrity assessment, and plastic collapse, as a consequence of unexpected high overloading, requiring the elastic-plastic analysis. Fatigue, corrosion and stress corrosion, and creep were not probable.

#### The application of linear elastic fracture mechanics

The application of LEFM is based on the stress intensity factor,  $K_I$ , representing loading and specimen geometry, including shape and size of the crack. Its critical value, plane strain fracture toughness,  $K_{Ic}$ , represents material characteristics. Based on these LEFM values and the energy criterion of Griffith, simple relations can be derived for a structural integrity assessment:

$$K_I \leq K_{Ic} \text{ - structural integrity is not critical (1a)}$$

$$K_I > K_{Ic} \text{ - structural integrity is critical, because of possible brittle fracture (1b)}$$

#### The analysis of critical defects by linear elastic fracture mechanics parameters

For the application of eq. (1) the stress intensity factor and the plane strain fracture toughness are required. Load and geometry are initial data for the determination of the stress intensity factor. It was not possible to determine fracture toughness, so conservative assumption of its value

is accepted. Special care was paid to residual stresses and stiffness due to the effect of the lid or the connections.

**Defect 970-64.** The data important for the analysis of the defect 970-64 are:

- vessel geometry (wall thickness  $t = 50$  mm, middle section diameter  $D = 2150$  mm);
- material of vessel mantle (NIOVAL 50 – low alloyed steel of 500 MPa yield stress);
- surface crack geometry (length 60 mm, width 2 mm, direction – along weld, position – root of longitudinal weld metal close to the circumferential welded joint between the mantle and the lid);
- loading (inside pressure  $p = 8.1$  MPa, residual stress  $\sigma_R = 200$  MPa – maximum value perpendicular to the weld, based on the experience with similar steel and pressure vessel [12]);
- weld metal fracture toughness  $1580 \text{ MPa}\sqrt{\text{mm}}$ , taken as a minimum value according to Ref. [13].

The defect 970-64 was considered as a surface crack extended along the total length of the cylinder for a conservative assumption, presented in the cross section perpendicular to the longitudinal axis (Fig.2). The dimension of the crack, accepted as its length (60 mm) was no more relevant, and the dimension used as width became the length for the analysis (2 mm). The effect of the curvature and the asymmetry of the crack location (22 mm from the lower plate side and 26 mm from its upper side) were neglected, that is reasonable for a thickness of 50 mm and 2150 mm diameter. In this way the problem was reduced to the tensile plate, with the dimensions much bigger than the crack length.

Taking remote stress as circumferential stress of pressure (boiler formula) increased for residual stress, acting across the weld middle, the stress intensity factor can be calculated as:

$$K_I = \left( \frac{pR}{t} + \sigma_R \right) \sqrt{\pi a} = \left( \frac{8.1 \cdot 1075}{50} + 200 \right) \sqrt{\pi \cdot 2} \quad (2)$$

$$= 663 \text{ MPa}\sqrt{\text{mm}}$$

Having in mind that the obtained value of  $K_I$  is 42% of the accepted minimum  $K_{Ic}$  value ( $1580 \text{ MPa}\sqrt{\text{mm}}$ ) one can conclude that brittle fracture is not possible. Even for the double crack size (covering uncertainty in measurement),  $K_I$  of  $937 \text{ MPa}\sqrt{\text{mm}}$  is only 59% of the accepted minimum  $K_{Ic}$  value.

**Defect 978-14.** Supposing that this defect in the circular weld joining bottom lid can be presented as a surface crack in the cross section normal to the circumferential direction (lack of penetration 25 mm long and 2 mm wide), extended along the full circumference of the pressure (Fig.3). The presented section is simplified, because the part belonging to the lid is also taken as flat, which is allowed neglecting of the curvature effect. The asymmetry, caused by the crack location, is neglected too. In addition, the fact that stress distribution in the torical part differs from the stress in the cylindrical part is neglected, because this stress is compressive and represents no danger to crack development. The additional data for this defect (basic data for material are already given above) are:

- vessel geometry (wall thickness  $t = 42$  mm, middle section diameter  $D = 1958$  mm);
- surface crack geometry (length 25 mm, width 2 mm, direction – along weld, position – root of weld metal of the circumferential welded joint with the lid, far from the connections);

- loading (inside pressure  $p = 7.8$  MPa, residual stress  $\sigma_R = 200$  MPa – as for defect 970-64).

Taking remote stress as axial stress due to pressure increased by transverse residual stress in the weld middle, the stress intensity factor is:

$$K_I = \left( \frac{pR}{2t} + \sigma_R \right) \sqrt{\pi a} = \left( \frac{7.8 \cdot 979}{100} + 200 \right) \sqrt{\pi \cdot 2} \quad (3)$$

$$= 515 \text{ MPa}\sqrt{\text{mm}}$$

presenting 32% of the critical value ( $K_{Ic} = 1580 \text{ MPa}\sqrt{\text{mm}}$ ), indicating that the pressure vessel is not critical. For a double crack size the calculated value is  $K_I = 728 \text{ MPa}\sqrt{\text{mm}}$ , presenting 45%  $\cdot K_{Ic}$ .

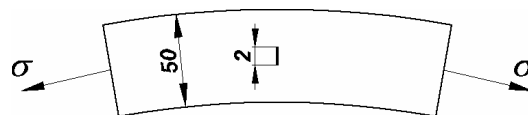


Figure 2. Cross section with the defect 970-64

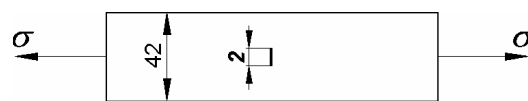


Figure 3. Cross section with the defect 978-14

**Defect 971-15.** This defect is presented in extremely conservative simplification as linear through crack, in the tensile panel, derived as a part of the pressure vessel mantle middle (Fig.4), because the second dimension of 10 mm overlapping in the circular weld is not known. The additional data (material is as in previous cases) are:

- vessel geometry (wall thickness  $t = 50$  mm, middle section diameter  $D = 2075$  mm);
- through crack geometry (length 10 mm, direction – along weld, position - circular weld metal in the vessel middle, far from the connections);
- loading (inside pressure  $p = 8.1$  MPa, residual stress  $\sigma_R = 175$  MPa – normal to the weld, out of the weld center, based on the experience with similar material and vessel [12]).

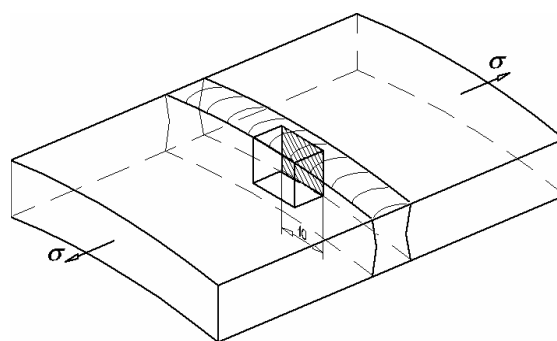


Figure 4. Scheme of the vessel mantle part containing the defect 971-57

Calculated again with axial stress and transverse residual stress, the stress intensity factor is:

$$K_I = \left( \frac{pR}{2t} + \sigma_R \right) \sqrt{\pi a} = \left( \frac{8.1 \cdot 1075}{100} + 175 \right) \sqrt{\pi \cdot 5} \quad (4)$$

$$= 1039 \text{ MPa}\sqrt{\text{mm}}$$

that is 66% of the critical value ( $K_{Ic} = 1580 \text{ MPa}\sqrt{\text{mm}}$ ). This value cannot produce brittle fracture. Even for a double crack size ( $K_I = 1465 \text{ MPa}\sqrt{\text{mm}}$  for  $2a = 20$  mm) it is lower than the critical value (92%).

The conclusion is that defective pressure vessels are safe regarding brittle fracture, under condition that no crack growth mechanisms exist.

#### The application of elastic-plastic fracture mechanics

Structures produced of materials with significant capacity for plastic deformation are not prone to brittle fracture, but can be exposed to plastic collapse when overloaded. The developed methods for the elastic-plastic analysis in structural integrity assessment are based on the crack tip opening displacement (CTOD), very attractive due to its simplicity, or the J integral, an energy parameter offering more detailed results due to solid theoretical bases, but more complex for application.

#### Failure analysis diagram - FAD

The two-parameter approach in the Failure Analysis Diagram (FAD) [3] enables definition of the limit line which separates the regions of safe and unsafe behaviour (Fig.5). This line is obtained applying a modified Dugdale's model of the yielded bands for the through crack in the infinite plate [6]:

$$\frac{K_{eff}}{K_I} = \frac{\sigma_c}{\sigma} \left[ \frac{8}{\pi^2} \ln \sec \frac{\pi}{2} \frac{\sigma}{\sigma_c} \right]^{1/2} \quad (5)$$

where  $K_I = \sigma \sqrt{\pi a}$ ,  $K_{eff}^2 = \delta \sigma_y E$ ,  $\delta$  is the crack tip opening displacement,  $E$  is the elasticity modulus, and the yield stress  $\sigma_y$  being replaced by the collapse stress (flow stress)  $\sigma_c$ , as a more convenient parameter for real structures. In the final stage dimensionless values are defined  $S_r = \sigma/\sigma_c$  and  $K_r = K_I/K_{Ic}$  for the FAD axes. In practical application  $K_{eff}$  is accepted as equal to the fracture toughness  $K_{Ic}$ , so the limit line is:

$$K_r = S_r \left[ \frac{8}{\pi^2} \ln \sec \left( \frac{\pi}{2} S_r \right) \right]^{1/2} \quad (6)$$

for the full plastic collapse  $S_r = 1$ , and for the brittle fracture  $K_r = 1$ . In all other situations the interaction between the plastic collapse and the brittle fracture exists, producing  $K_r$  and  $S_r$  less than 1. The pairs of corresponding values according to Eq. (6) form the limit line (Fig.5).

The stresses, necessary for the determination of  $K_r$  and  $S_r$ , are defined in [3] or in [4] as primary and secondary (residual). For the determination of  $S_r$  only primary stresses are applied, since secondary stresses can not produce plastic deformation and collapse.

It is to be mentioned that the application of the FAD is not restricted to the stress intensity factor  $K$ , also the J integral or the COD ( $\delta$ ) can be used. The presented FAD form corresponds to a simplified level "I", but more detailed levels "II" and "III" are described in [3] and in [4]. The presented level "I" approach is applied here to the previously considered defects. The parameter  $K_r$  is already known (0.59 for the defect 970-64, 0.45 for the 978-14 and 0.92 for the 971-57).

The stress caused by pressure (primary stress) in the net section is only necessary for the determination of  $S_r$  parameter. The stress for the defect 970-64 is  $\sigma_n = 1.08 pR/t$ , with the factor 1.08 taken for the thickness of 50 mm weakened in the net section by the 4 mm long crack (8%), so:

$$S_r = \frac{\sigma_n}{\sigma_c} = 2 \frac{1.08 pR}{R_{eH} + R_m} = 2 \frac{1.08 \cdot 8.1 \cdot 1075}{500 + 650} = 0.33 \quad (7a)$$

The data for the yield stress  $R_{eH}$  (500 MPa) and the tensile stress  $R_m$  (650 MPa) are taken from the design specifications for base metal, and the values for weld metal are close to them. The effect of the lid is neglected, since this defect produces stress change in the torical part, but not in the cylindrical mantle.

The stress for the defect 978-14 is  $\sigma_n = 1.05 pR/t = 95$  MPa, with the factor 1.05 for the thickness of 42 mm weakened in the net section by the 2 mm long crack (8%), so:

$$S_r = \frac{\sigma_n}{\sigma_c} = \frac{95}{575} = 0.17 \quad (7b)$$

The effect of the lid is also neglected.

The stress for the defect 971-57 is  $\sigma_n = pR/t = 87$  MPa, the cross section is not weakened, so:

$$S_r = \frac{\sigma_n}{\sigma_c} = \frac{87}{575} = 0.15 \quad (7c)$$

Based on the obtained values for  $K_r/K_{Ic}$  and  $\sigma_n/\sigma_c$  the pairs of coordinates are calculated (0,33; 0,59) (0,17; 0,45) and (0,15; 0,92), and presented in the FAD (Fig.5). All points are in the safe region.

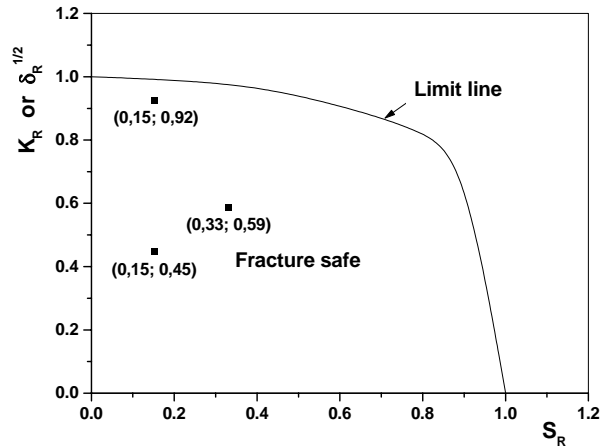


Figure 5. Failure Analysis Diagram - FAD for the considered defects on pressure vessels

The performed analysis is conservative in all aspects and enabled the conclusion that the defective pressure vessels are safe not only regarding brittle fracture, but also regarding plastic collapse. It is to notice that the FAD approach allows a simple structural integrity analysis of components if the geometry and loading are applied in the conservative way. On the other hand, if structural integrity is not proved in this way it does not automatically mean that the component is not usable, but that further, more complex analyses are required before the final decision.

#### Crack growth analysis by J integral

Two aspects of the J integral have to be considered for structural integrity assessment. In the first one, the J integral is an elastic-plastic fracture mechanics parameter, which defines the cracked body geometry and loading (crack driving force - CDF), and in the second it represents crack resistance of material ( $J_{Ic}$  and J-R curve) [14]. The fundamental difference in these two aspects is the crack growth behaviour. In the first case the crack size is not variable and together with stress is used as parameter. In the second case the crack growth is included. The criterion for the initiation of the stable crack growth is:

$$J(\sigma, a) \geq J_{Ic} \quad (8)$$

where  $J(\sigma, a)$  is the crack driving force (CDF), dependent on the remote stress (loading)  $\sigma$  and crack length (size)  $a$ , whereas  $J_{Ic}$  is the material resistance to the initiation of the stable crack growth. The crack growth analysis in the elastic-plastic fracture mechanics is not restricted to the application of Eq. (8), but also involves the stable crack growth and the condition for the initiation of its unstable extension, e.g. J-R curve, which is compared to the CDF by a convenient graphical presentation (Fig.6). The mathematical formulation for the initiation of the unstable crack growth is given by:

$$\frac{\partial J(\sigma, a)}{\partial a} \geq \frac{\partial J}{\partial a} \quad (9)$$

indicating that the increase in the CDF must be greater than the increase of the material crack resistance for the same crack extension. So, when the value  $J(\sigma, a)$  reaches the value  $J_{Ic}$  (Eq. 8, intersection of the CDF curve and the J-R curve), the stable crack growth initiates and continues up to the instant in which  $\partial J(\sigma, a)/\partial a$  becomes greater than  $\partial J/\partial a$  (Eq. 9, tangent of CDF curve to the J-R curve) producing unstable crack growth (Fig.6). The stable crack growth extent  $\Delta a$  is determined as the difference (on the abscissa) of the described points  $A$  and  $a_o$ , including the crack tip blunting.

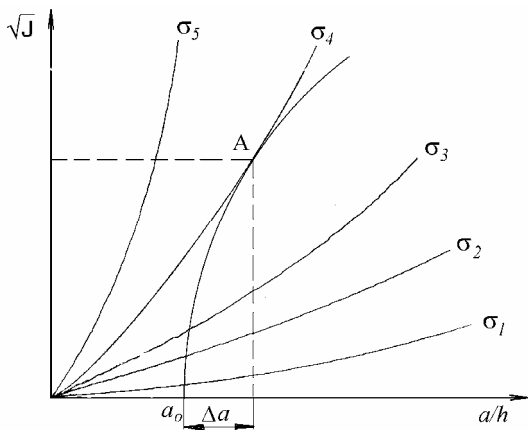


**Figure 6.** Crack driving force (CDF) in parametric dependence on the applied stress  $\sigma$  vs. the J-R curve

In practical application the CDF can be determined by a convenient theoretical-analytical model, such as the Ratwani-Erdogan-Irwin (REI) model [15], [16], King's line spring model [17], or numerically, by finite elements method (FEM). Crack resistance can be determined experimentally, e.g. according to ASTM E1820 [18] or applying the J integral direct measurement method [19].

#### Verification of the residual strength (structural integrity) assessment method

For conservative prediction of residual strength and structural integrity of a cracked welded structure, the maximum crack driving force is compared to the minimum material crack resistance. In order to prove that the applied model for residual strength prediction is conservative, the experimental pressure vessel (Fig.7, I) was welded of high-strength low-alloyed steel SM80P (700 MPa nominal yield strength) 16 mm thick (Sumitomo, Japan), by a qualified submerged-arc-welding (SAW) procedure, and prepared for

the verification of the REI model conservatism [20], using the J integral direct measurement [19] on the WM sample (Fig.7, II). The sample 180x380 mm, containing weld metal, was cut from a welded prototype. After machining the notch in the weld metal, a fatigue pre-crack was produced, and the sample was re-welded on the pressure vessel. A properly selected contour DCBAB'C'D", (Fig.7, III), enabled the J integral direct evaluation by measuring the strains on the regularly distributed strain gauges (Fig.7, IV), and the COD by the clip gauge. It is interesting that during the experiment the crack developed in length, from the initial value  $2c = 64.25$  mm up to 72 mm after the first stage and the final value of 80 mm, as measured after the experiment, and did not develop in depth (Fig.7, II).

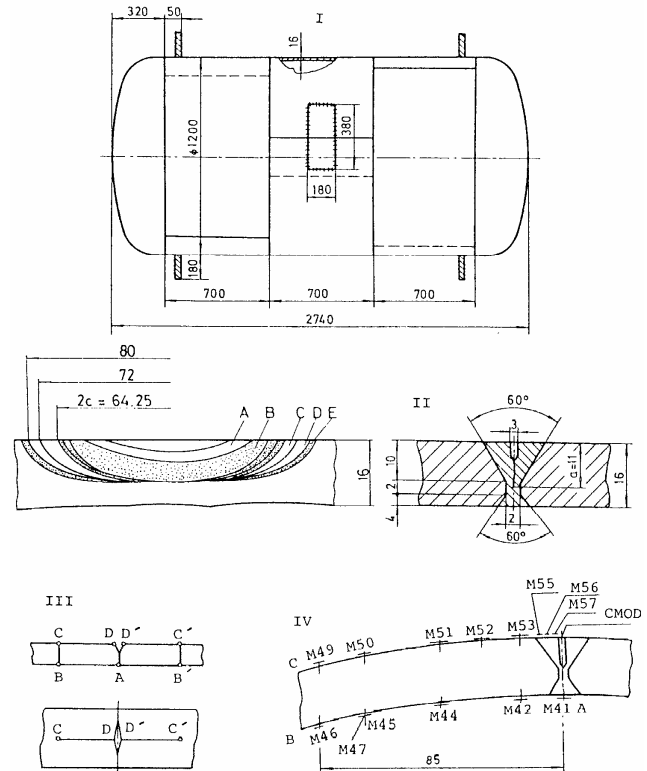


**Figure 7.** I Experimental pressure vessel; II Detail of the crack; III Integration path; IV Distribution of the strain gauges. (A notch; B fatigue pre-crack; C,D stable crack growth; E final fatigue)

For the crack length  $2c = 64.25$  mm and the mid-thickness shell radius  $2R = 1184$  mm, the wall thickness  $W = 16$  mm, Poisson's ratio  $\nu = 0.3$ , the shell parameter  $\lambda$  necessary for the following calculation, is:

$$\lambda = [12(1-\nu^2)]^{1/4} = [12(1-0.3^2)]^{1/4} \frac{32.125}{\sqrt{1184 \cdot 0.016}} = 0.6$$

he crack driving forces for an axial surface crack in the pressure vessel have been calculated by the REI model for this value of the shell parameter and expressed by a set of lines in Fig.8, depending on the crack ratio  $a/W$  and the normalized pressures  $pR/WR_{p0.2}$  ( $p$  is the applied pressure,  $R_{p0.2}$  is the yield stress of the weld metal). The point "A" is experimentally obtained at a pressure of 100 bar for the crack depth, measured after testing ( $a = 11$  mm, crack ratio  $a/W = 0.69$ ). For the same pressure the crack driving force, corresponding to  $a/W = 0.69$ , is higher for 40% than the point "A", indicating that the applied crack driving force is significantly lower than the value obtained, and that The REI model is conservative.

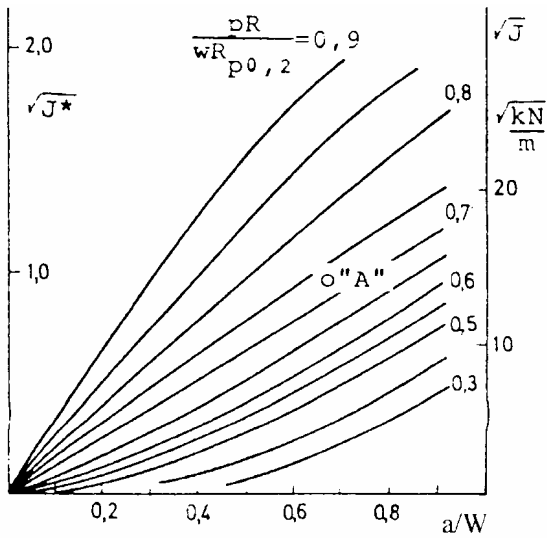


Figure 8. Set of the crack driving forces with the implemented point "A", obtained by the J integral direct measurement on the experimental pressure vessel

Application of the J – R curves for the structural integrity assessment

The next problem in the structural integrity assessment is how to obtain the crack resistance (J-R) curve. In this experiment the SEN type of specimen is selected (Fig.9, I) for the single specimen technique proposed in ASTM E1820 [18], applying successive unloading for crack growth measurement. In addition, the instrumented tensile panels with surface cracks (Fig.9, II) were tested by the J integral direct measurement method [19]. In both specimen types the cracks were positioned in the base metal, the weld metal and the heat-affected zone (HAZ). A typical crack located in the HAZ of the tensile panel is given in Fig.9, III as an example. The cross section of the tensile panel (75x15 mm) was weakened by a large crack (24 mm long, 5 mm deep) and by a small crack (16 mm long, 2.5 mm deep).

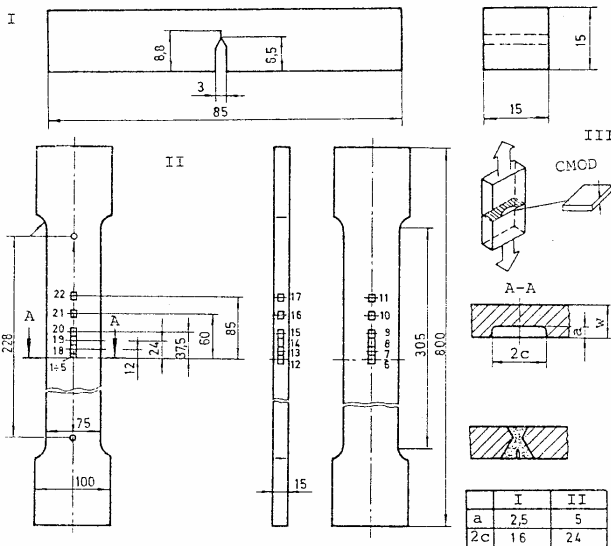


Figure 9. Pre-cracked specimens (I - three point bend specimen; II - tensile panel, III - details of the surface cracks on the tensile panels)

Two typical plots load vs. the crack opening displacement, obtained by the single specimen compliance technique of the tensile panels and the SEN(B) specimens, are presented in Fig.10. In general, they are of a regular shape, Fig.10, I. Only for few SEN(B) specimens, with the

crack positioned in the HAZ, declining occurred, indicating a fast crack growth ("pop-in" presented in Fig.10, II).

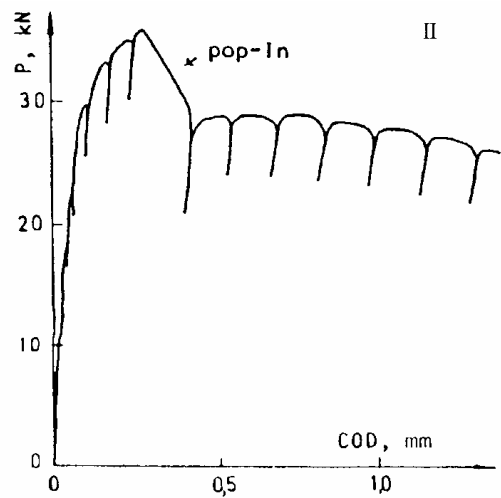
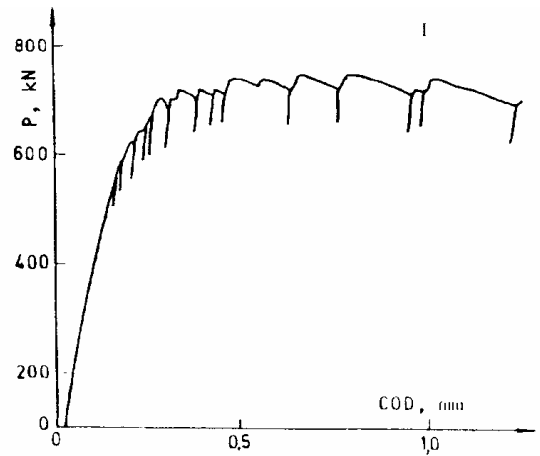


Figure 10. Typical plots load P vs. crack opening displacement COD for cracks in the HAZ (I - tensile panel; II - three point bend single specimen compliance technique - arrow indicates "pop-in")

The high-strength low-alloy steel SM80 was the base material in this experiment. The welded joints of the SM80 steel were produced as normal matched, applying consumable producing weld metal of slightly lower strength compared to the base metal. The crack growth resistance of the welded joint constituents is expressed through the J-R curves for the base metal (BM) SM 80P and for the weld metal (WM) in Fig.11, and for the HAZ of the normal matched weldment of the SM 80P steel in Fig.12.

The slope of the J-R curve for the SM 80P steel indicates good properties regarding the crack growth (Fig.11, I). The agreement of the results obtained with the SEN(B) specimens and the tensile panels is obvious. The high crack resistance of this steel is obtained even at a significant crack ratio ( $a/W = 0.61$ ).

The crack growth resistance of BM and WM is similar only for small cracks in the base metal (Fig.11, I, for  $a/W=0.15$ ,  $a/W=0.31$ ) and in the normal matched weld metal in the tensile panel (Fig.11, II,  $a/W=0.19$ ). In other cases the crack growth resistance of WM is lower when compared to the base metal.

Significant differences in the crack growth resistance (Fig.12) are caused by heterogeneity of the heat-affected-zone microstructure, but also by a specimen type. For

$a/W=0.14$  ratio in tensile panel crack growth resistance of the HAZ and BM are of similar value, but this is not the case when the SEN(B) specimens with a small crack ratio are considered, where in two cases, for  $a/W=0.21$  and  $a/W=0.20$ , a so called "pop-in" in the crack growth was observed (Fig.12, II), indicating that the through crack can develop more easily than the surface crack in the tensile panel (compare the crack behaviour in Fig.7). Even in that case the satisfactory agreement of results for both specimen types (tensile panel and SEN(B) specimen) with the same crack ratio is obvious. This property of the J-R curve is an additional reason for its acceptance as a general parameter of cracked specimen behaviour.

The crack driving force lines and the J-R curves for residual strength prediction are given in Fig.13. Some J-R curves for the WM are adopted from Fig.11. The lower scatter band for the HAZ, that takes into account the pop-in effect, could be accepted as representative from Fig.12.

The behaviour of the crack in the HAZ is close to critical mainly due to the expressed "pop-in" behaviour (Fig.10, Fig.12). The lower bound (LB) curve (Fig.13) has been accepted for the analysis because it covers all "pop-ins" noticed in the testing. For the crack ratio  $a/W=0.548$ , the crack depth is  $a_0=8.77$  mm and the pressure  $p = 120$  bar can produce the unstable crack growth for next 0.8 mm, before the crack tip reaches the region of tougher material in which the crack grows in stable manner.

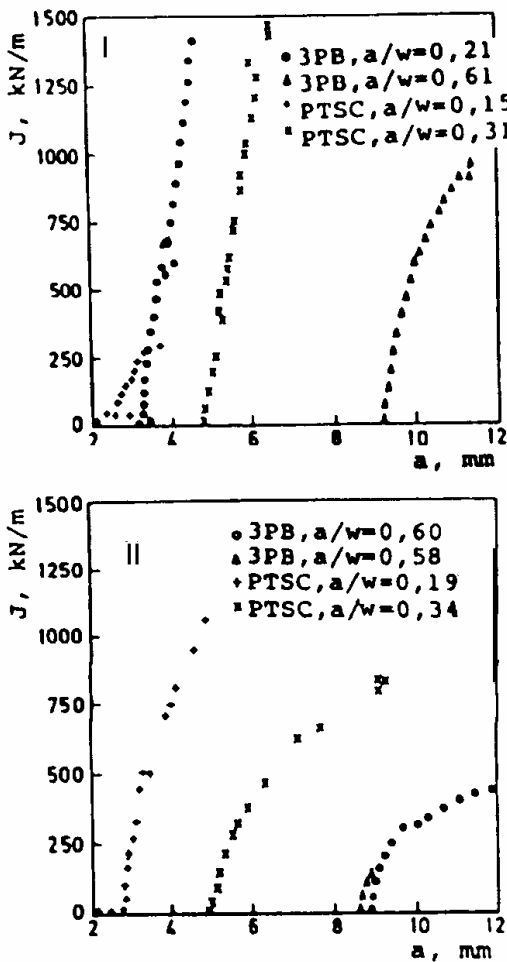


Figure 11. J-R curves: I-base metal SM 80P steel; II-designed normal matched welded joint (3PB - three point bend specimen, TPSC – tensile panel with the surface crack)

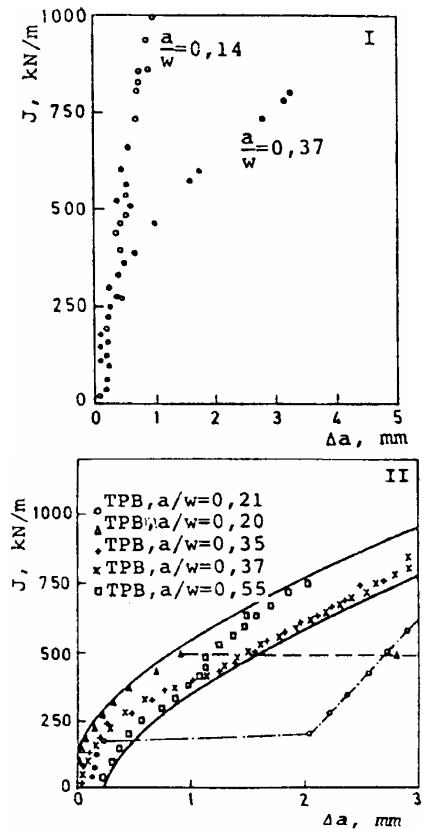


Figure 12. J-R curves for the crack in the heat-affected-zone (I-tensile panel; II-three point bend specimen)

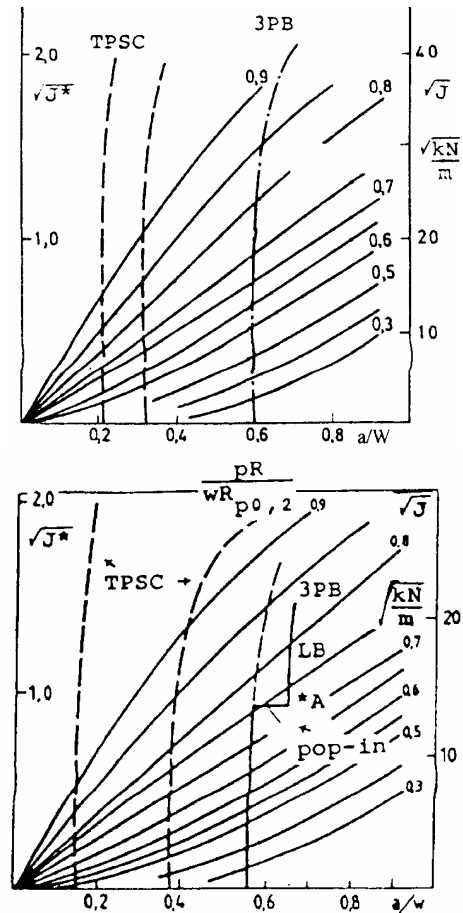
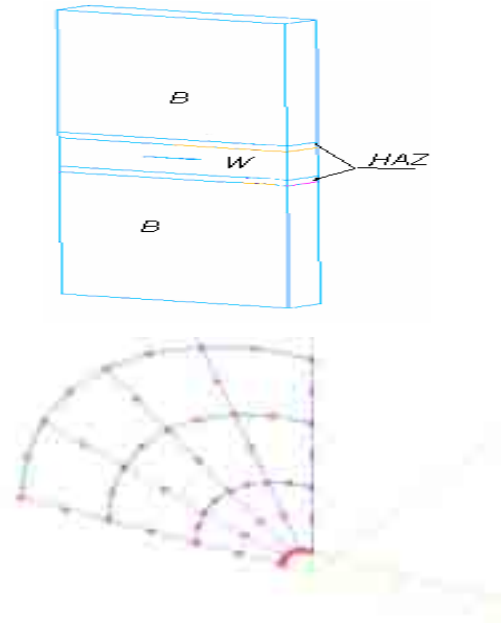


Figure 13. Residual strength estimation for the pressure vessel cracked in the WM (TPSC-tensile panel with surface crack; 3PB-three point bend) - left, and in the HAZ (LB - lower bound for 3PB specimens) - right

The pressure of 120 bar can be reached in this structure, but the situation cannot be judged as critical, because the crack of a given size is not probable in real structures and even smaller cracks could be easily detected by modern equipment for non-destructive testing.

*The finite element modelling of THE cracked welded plate*

The first step was a modeling plate with a surface crack with a wire model, Fig.14a, and then a model with a coarse mesh was designed. The crucial region in this process is the weldment of heterogeneous metal, with the crack, requiring a fine and non-uniform mesh, Fig.14b. The models comprising regions with different microstructural properties are discretized accordingly for separate analyses of weld metal, HAZ and base metal. This is achieved by an appropriate mapping contour in the plate (Fig.15).



**Figure 14.a.** Wire model – left. b. Mesh around the crack tip -right

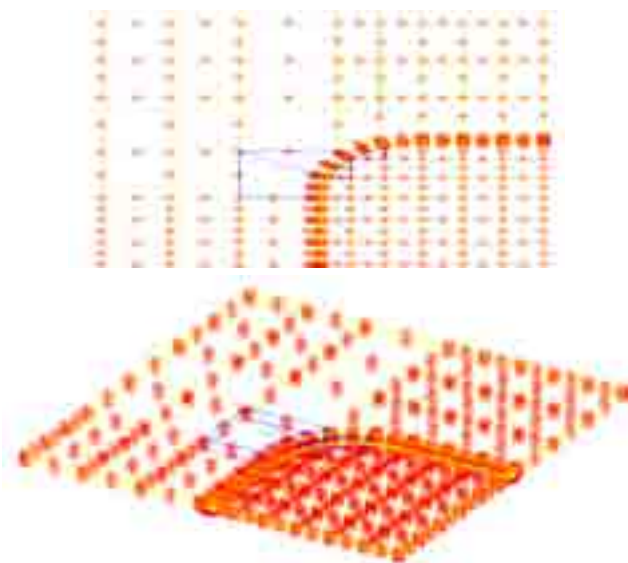
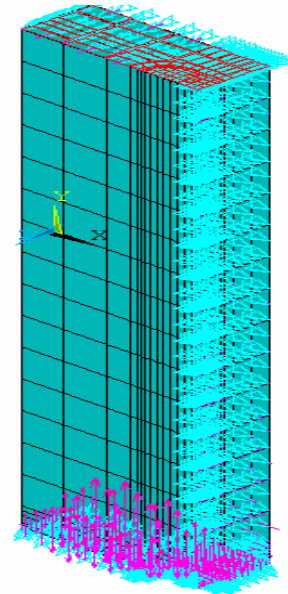


**Figure 15.** Mapping contour for the surface crack in the plate

The region with the crack required a special manual and semi-manual procedure. The first 2D eight-noded (thin shell) elements were generated, which were then "deformed" to take the singularity into account, i.e. to form the crack tip and the model elastic-plastic behaviour at the same time, Fig.15. Then, on the basis of these plane elements, the 3D region of the elastic-plastic singularity has been formed. Finally, after 3D singular elements formed the crack front, they are merged with the surrounding uniform mesh, consisting of hexaedric elements (standard 20 noded element).



```

SEP 26 2004
09:56:45
NODAL SOLUTION
STEP=2
SUB =100
TIME=2000
SEQV (AVG)
PowerGraphics
EFACET=1
AVRES=Mat
DMX =.491E-03
SMN =.112E+09
SMX =.805E+09
.112E+09
.189E+09
.266E+09
.343E+09
.420E+09
.497E+09
.574E+09
.651E+09
.728E+09
.805E+09
    
```

**Figure 16.** Boundary conditions for the plate

The results for the strains along the J integral contour are shown in Fig.17 for the undermatched welded joint and in Fig.18 for the overmatched welded joint, together with the experimental results. Good agreement between numerical and experimental analysis is achieved.



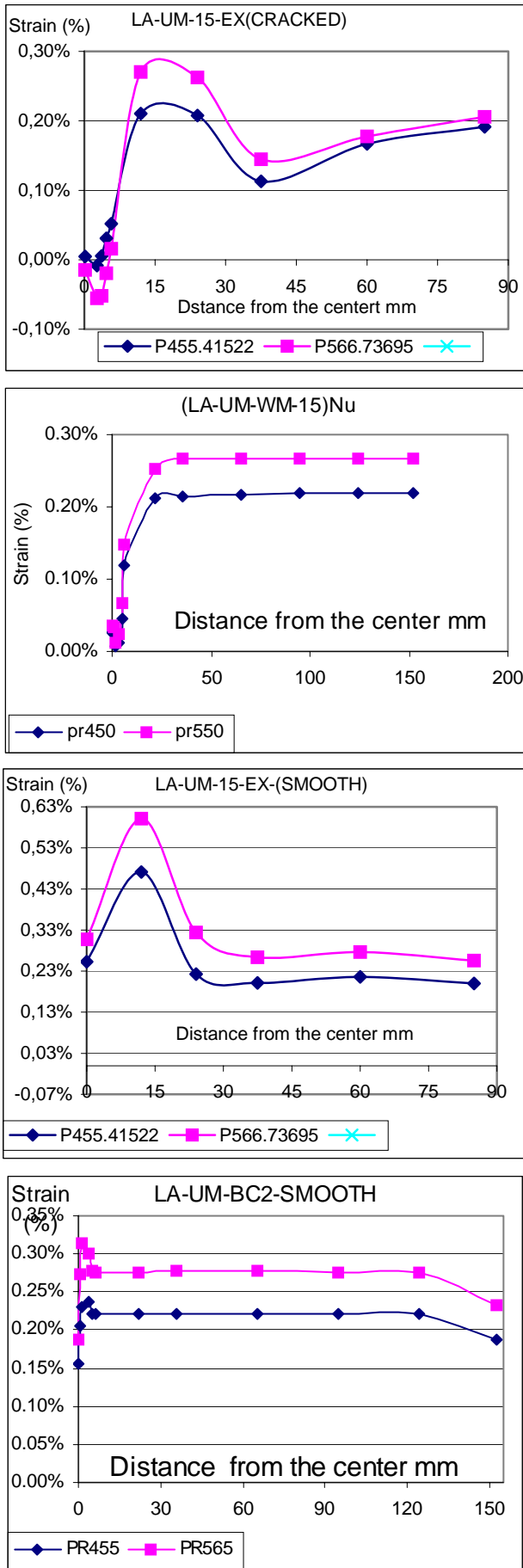


Figure 17. Comparison between the numerical and the experimental results for the undermatched weld

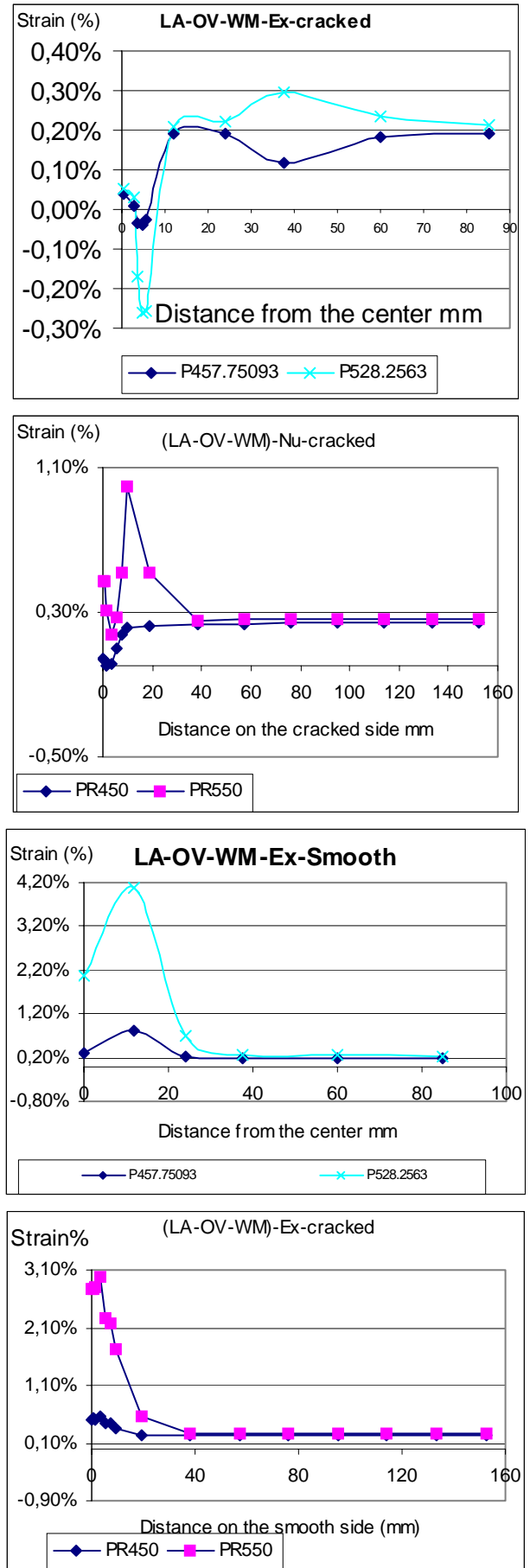


Figure 18. Comparison between the numerical and the experimental results for the overmatched weld

## Conclusions

The introduction of fracture mechanics basically changed engineering practice, accepting possibility of crack and crack-like defects existence and necessity to analyze their effect on structural integrity.

The practical application of fracture mechanics to the structural integrity assessment is presented and considered for three different cases of welded structures. The danger of brittle fracture is assessed by the basic linear elastic fracture mechanics formulae for the stress intensity factor, with necessary simplification in order to save the conservatism of the applied method. Applying the elastic-plastic fracture approach from PD 6493, again with allowed simplifications, it is shown that structural integrity is not questionable and that necessary conservatism in assessment is saved. In both cases the response to the question of structural integrity of the considered defective pressure vessels is positive, proving that their further service is possible with no additional repair. The heterogeneity of the welded joints is not considered, because the approach is conservative and takes only the worst case situation.

For a detailed analysis of cracks in welded joints the application of the J integral could be significantly better, as it is possible to conclude from the presented examples. Anyhow, microstructural heterogeneity, followed by heterogeneity of mechanical properties and crack resistance of different regions in the HAZ, requires even a more detailed analysis. This is possible to achieve by the HAZ simulation and determination of properties of different microstructures in the HAZ. But even then the scale effect has to be taken into account, because the behaviour of a crack in real structures and in specimens can be different.

Heterogeneous microstructure of welded joints containing cracks cannot be described completely by theoretical and experimental analyses, and the additional numerical analysis, e.g. the finite elements method (FEM) is necessary and can help significantly in understanding differently matched weld metals containing cracks. This is confirmed by the given examples of the FEM for undermatched and overmatched weldments.

## References

- [1] NICHOLS,R.W.: (1984), The use of fracture mechanics as an engineering tool. The 1984 ICF Honour Lecture. Sixth International Conference on Fracture, ICF 6, New Delhi, India.
- [2] SEDMAK,S.: (1985), The evaluation of welded joint properties by testing of precracked specimens, The monograph Fracture Mechanics of Weldments, ed. S Sedmak), GOŠA, TMF, Beograd, 281-306 (in Serbian)

- [3] PD 6493 (1996), *Guidelines on some methods for the derivation of acceptance levels for defects in fusion welded joints*, BSI, London
- [4] SINTAP: *Structural Integrity Assessment Procedure* (1999). Final Report. EU-Project BE 95-1462. Brite Euram Programme, Brussels.
- [5] GUBELJAK,N., ZERBST,U.: (2004), *SINTAP- Structural Integrity Assessment Procedure*, The monograph From fracture mechanics to structural integrity assessment, ed. Z. Radaković and S. Sedmak, DIVK, TMF, Beograd, 303-320
- [6] BURDEKIN,F.M. and DAWES,M.G.: (1971), *Practical use of linear-elastic and yielding fracture mechanics with particular references to pressure vessels*, IIW Document X-641-71.
- [7] BURDEKIN,F.M.: (1982), *The assessment of critical crack size in pressure vessels*, The monograph Modern aspects of desing and manufacturing of pressure vessels and penstocks. ed. S. Sedmak, GOŠA, TMF, Beograd, 151-160 (in Serbian)
- [8] REED,R.P., MACHENRY,H.I., KASEN,M.B.: (1979), *A fracture mechanics evaluation of flaws in pipeline girth welds*, Welding Research Council Bulletin, No 245
- [9] SEDMAK,S., RADOVIĆ,A., NEDELKOVIĆ,L.J.: (1979) *The strength of welds in HSLA steel after initial plastic deformation*, in Mechanical Behaviour of Materials (Edited by K. J. Miller and R. F. Smith). Vol. 3. Pergamon Press, Oxford & New York, 435-446.
- [10] SATOH,K. AND TOYODA,M.: (1975), *Joint strength of heavy plates with lower strength weld metal*, AWS (Translation from Japanese)
- [11] *Internal reports* (1998), GOŠA Institute, S. Palanka
- [12] ADŽIEV,T., (1988), *A contribution to the effect of residual stresses on fracture resistance of cracked welded structure*, doctoral thesis, Mechanical Engineering Faculty,Skopje (in Macedonian)
- [13] GERIC,K., (1997), *Crack occurrence and development in welded joints of high strength steel*, doctoral thesis, Faculty of Technology and Metallurgy, Beograd (in Serbian)
- [14] BOZIĆ,B., SEDMAK,S., PETROVSKI,B., SEDMAK,A.: (1989), *Crack growth resistance of weldment constituents in a real structure*, Bulletin T. Cl de l'Academie serbe des Sciences at des Arts, Classe des Sciences techniques. No 25, Beograd, 21-24
- [15] ERDOGAN,F. and RATWANI,M.M.: (1972), *Plasticity and the crack opening displacement in shells*, Int. J. Fract. Mech. 8(4), 413-426
- [16] RATWANI,M.M., ERDOGAN,F., IRWIN,G.R.: (1974), *Fracture propagation in cylindrical shell containing an initial flaw*, Lehigh University, Bethlehem
- [17] KING,R.B.: (1983) *Elastic-plastic analysis of surface flaws using a simplified line-spring model*, Eng. Fracture Mech. 18, 217-231
- [18] ASTM E 1820 -99: Standard Test Method for Measurement of Fracture Toughness
- [19] READ,D.T.: (1983), *Experimental method for direct evaluation of the J contour integral*, ASTM STP 791, 199-213.
- [20] US-Yugoslav joint project "*Fracture mechanics of weldments*" (1982-1991), Annual reports, Faculty of Technology and Metallurgy, University of Beograd, Principal investigator S. Sedmak

Received: 05.12.2007.

## Procena integriteta posuda pod pritiskom sa greškom u zavarenom spoju

U radu su prikazani primeri primene parametara mehanike loma za procenu integriteta posuda pod pritiskom sa prslinom.

Primena parametara mehanike loma zavisi od niz podataka, pre svega o ponašanju materijala u prisustvu greške, uticaju okoline i opterećenja. U uslovima dominantnog statičkog opterećenja, ponašanje materijala sa greškom može biti opisano kao linearno-elastično, i bazira se na faktoru intenziteta napopna,  $K_I$ , pri čemu se plastična deformacija zanemaruje, dok u elasto-plastičnom području ponašanje materijala se definiše pomeranjem otvora prsline ili J integralom kao parametrima mehanike loma.

Linearno-elastična mehanika loma je primenjena za slučaj cilindričnog rezervoara za komprimovani gas kod koga su primenom metoda bez razaranja otkrivene nedozvoljene greške u zavarenim spojevima prema ISO 5817. Otkrivene greške su svedene na tip prsline u funkciji primene konzervativnog proračuna. Primenom faktora intenziteta napona u proceduri PD 6493 (Uputstvo o metodama izbora nivoa prihvatljivosti grešaka u zavarenim spojevima) se pokazalo da integritet analiziranih rezervoara nije narušen.

J integral je primenjen za analizu ponašanja u elsto-platičnom području. Posude pod pritiskom koje su predmet eksperimentalnog rada su izrađene zavarivanjem čelika sa granicom tečenja od 700MPa. Uticaj veličine prsline je određen upoređenjem sile za rast prsline (određena primenom Ratwani-Erdogan-Irwin modela) i eksperimentalno određene krive otpornosti materijala koja je definisan na bazi direktnog merenja J integrala..

Teoretska i eksperimentalna analiza ne definiše u potpunosti ponašanje zavarenih spojeva sa prslinom, kao i heterogenu mikrostrukturu u zoni spoja. Zbog toga, numerička analiza može biti korisna ukoliko se primeni na pravi način. U radu je prikazan i primer primene metode konačnih elemenata za analizu zavarenih spojeva.

*Ključne reči:* integritet konstrukcija, posude pod pritiskom, zavareni spoj, prsline, mehanika loma, faktor intenziteta napona, pomeranje vrha prsline, J integral.

## Evaluation de l'intégrité des récipients sous pression avec défaut de la soudure

Les exemples de l'application des paramètres de la mécanique de fracture pour évaluation de l'intégrité structurale des récipients sous pression avec fissure sont présentés dans ce travail. L'application des ces paramètres dépend d'une série de données, du comportement du matériel en présence du défaut, de l'influence de l'environnement et de la charge. Quand la charge statique est prédominante, le comportement du matériel avec défaut peut être décrit comme linéaire-élastique, basé sur le facteur d'intensité de la tension K, où la déformation plastique est négligée, alors que le comportement du matériel dans le domaine élastique-plastique se définit par le déplacement de l'ouverture de fissure ou par l'intégral I comme le paramètre de la mécanique de fracture. La mécanique de fracture linéaire élastique est appliquée chez le réservoir cylindrique pour le gaz comprimé, où l'on a trouvé, à l'aide des méthodes non-destructives, les défauts inadmissibles dans les soudures selon ISO 5817. Les défauts trouvés sont réduits en type de fissure en fonction de l'application d'évaluation conservative. Employant le facteur de l'intensité de tension selon la procédure PD 6493 (Instruction sur les méthodes du choix des niveaux d'acceptabilité des défauts chez les soudures), on a démontré que l'intégrité des réservoirs analysés n'est pas mise en danger. L'intégral I est employé pour analyser le comportement dans le domaine élastique-plastique. Les récipients sous pression qui faisaient l'objet des essais, étaient produits par le soudage de l'acier à limite d'écoulement de 700 MPa. L'analyse théorique et expérimentale ne définit pas complètement des soudures avec fissure et la microstructure hétérogène dans la zone de soudure. Pour cette raison, l'analyse numérique est utile si elle est faite à bon escient. Dans ce travail on a donné aussi un exemple de l'application de la méthode des éléments finis pour l'analyse des soudures.

*Mots clés:* intégrité de structure, récipients sous pression, soudure, erreur de soudure, fissure, mécanique de fracture, état de tension, intégral, méthode des éléments finis.